A Spectroscopic and Calorimetric Investigation on the Thermal Stability of the Cys3Ala/Cys26Ala Azurin Mutant

R. Guzzi,* L. Sportelli,* C. La Rosa,# D. Milardi,# D. Grasso,# M. Ph. Verbeet,§ and G. W. Canters§

*Dipartimento di Fisica e Unità INFM, Laboratorio di Biofisica Molecolare, Università della Calabria, 87030 Rende (CS), Italy, #Dipartimento di Scienze Chimiche, Università di Catania, Viale A. Doria, 95125 Catania, Italy, and §Leiden Institute of Chemistry, Gorleaus Laboratories, Leiden University, P.O. Box 9502, 2300 RA Leiden, The Netherlands

ABSTRACT The disulfide bond connecting Cys-3 and Cys-26 in wild type azurin has been removed to study the contribution of the –SS– bond to the high thermal resistance previously registered for this protein (La Rosa et al. 1995. *J. Phys. Chem.* 99:14864–14870). Site-directed mutagenesis was used to replace both cysteines for alanines. The characterization of the Cys-3Ala/Cys-26Ala azurin mutant has been carried out by means of electron paramagnetic resonance spectroscopy at 77 K, UV-VIS optical absorption, fluorescence emission and circular dichroism at room temperature. The results show that the spectral features of the Cys-3Ala/Cys-26Ala azurin resemble those of the wild type azurin, indicating that the double mutation does not affect either the formation of the protein's overall structure or the assembly of the metal-binding site. The thermal unfolding of the Cys-3Ala/Cys-26Ala azurin has been followed by differential scanning calorimetry, optical absorption variation at $\lambda_{max} = 625$ nm, and fluorescence emission using 295 nm as excitation wavelength. The analysis of the data shows that the thermal transition from the native to the denaturated state of the modified azurin follows the same multistep unfolding pathway as observed in wild type azurin. However, the removal of the disulfide bridge results in a dramatic reduction of the thermodynamic stability of the protein. In fact, the transition temperatures registered by the different techniques are down-shifted by about 20°C with respect to wild type azurin. Moreover, the Gibbs free energy value is about half of that found for the native azurin. These results suggest that the disulfide bridge is a structural element that significantly contributes to the high stability of wild type azurin.

INTRODUCTION

One of the most puzzling problems in biochemistry is how a polypetide chain, which is synthesized as a linear heterogeneous polymer, folds into a functionally unique three-dimensional structure. In this respect, the knowledge of the energetics of protein folding/unfolding is crucial to our understanding of the formation and functioning of protein molecules (Privalov, 1992). The stability of the native conformation of proteins is the result of all noncovalent interactions between backbone and side chain atoms, the covalent interchain disulfide bonds, and the coordinative bond between the metal ion and the protein side chains that act as ligands in all metallo-proteins. It has been shown that the integrity of the native three-dimensional structure of many proteins is promoted by the presence of disulfide bridges, because the removal of one or more of these bridges results in a reduction in the stability of the native relative to the denatured state (Creighton, 1974; White, 1982; Wetzel et al., 1988; Taniyama et al., 1988; Inaka et al., 1991; Cooper et al., 1992). Consequently, the investigation of the role of disulfide bonds for the stability of folded proteins has received a lot of attention. Protein engineering techniques have been recently employed in the attempts to increase both the overall stability of proteins by the introduction of non-native disulfide linkages into the structure and as specific probes of the folding pathway (Creighton, 1992; Clarke and Fersht, 1993). Although in some cases, the increase of the stability of a mutated protein relative to the wild type (wt) form has been observed, this is not generally the case (Wetzel, 1987; Matsumura et al., 1989). Many factors, including the location of the mutation site, the loop size connected by the –SS– linkage, and the strain energy introduced by the disulfide bridge, have to be considered to estimate the effect on the protein stability (Matsumura et al., 1989; Vogl et al., 1995). The mechanism of protein stabilization by disulfide bridge formation is difficult to resolve because the –SS– bond may influence enthalpy and entropy of both the native and unfolded state of the protein. In this respect, the two approaches commonly used are the introduction of artificial disulfide bridges (Clarke and Fersht, 1993; Gokhale et al., 1994; Tamura et al., 1994) and the removal of natural disulfide bonds either through Cys replacement by genetic engineering techniques or by opening existing disulfide bridges by chemical reduction (Schwarz et al., 1987; Pace et al., 1988; Cooper et al., 1992).

The generality of these concepts has been tested on azurin, a small blue copper protein belonging to the cupredoxin family, that acts as an electron transfer shuttle in the redox systems of certain bacteria. This protein has 128 amino acid residues and one copper(II) ion with Gly-45, His-46, Cys-112, His-117, Met-121 as metal ligands. The structure of wt azurin, that has been resolved by x-ray diffraction study (Nar et al., 1991), consists of eight β-strands that form two sheets in a Greek-key motif (Fig. 1). This is the common fold in the cupredoxin family. In azurin,

Received for publication 10 November 1998 and in final form 3 May 1999.

Address reprint requests to Dr. Luigi Sportelli at Dipartimento di Fisica, Università della Calabria, Arcavacata di Rende, 87030 Rende (CS), Italy. Tel.: 39–0984-493073; Fax: 39–0984-493187; E-mail: sportelli@fis.unical.it.

0006-3495/99/08/1052/12 $2.00

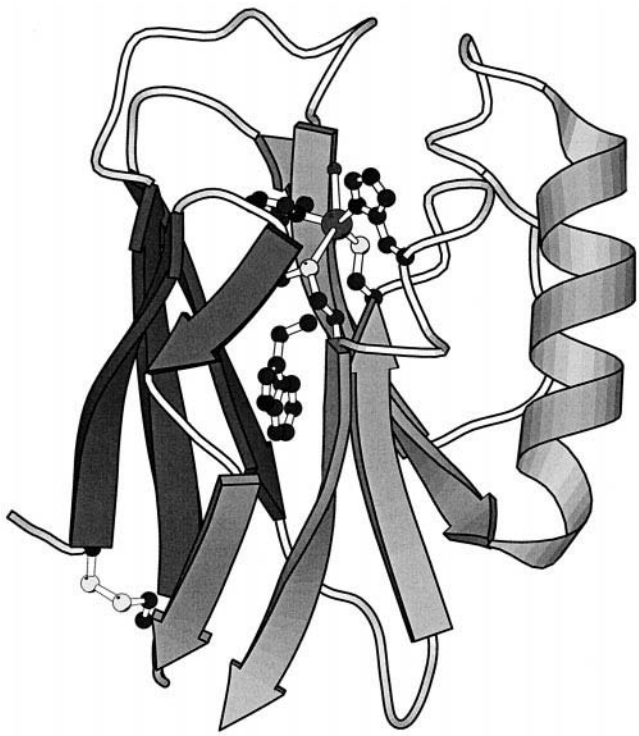

FIGURE 1 Model of wt azurin generated with Molscript program (Kraulis, 1991). The figure shows the copper ion with its ligands (*top*), the Trp-48 residue (*middle*), and the disulfide bridge (*bottom*).

the two sheets are connected by an α-helix at one side and by a kink in one of the β-strands at the other side. A disulfide bridge connecting Cys-3 and Cys-26 is present at the southern end of the protein. Azurin has only one tryptophan residue, Trp-48, pointing with its side chain to the center of the hydrophobic core.

It is generally recognized that the stability of the cupredoxins does not depend on the presence of the disulfide bridge. In fact, other members of the cupredoxin family, such as plastocyanin (Guss et al., 1992) and amicyanin (Kalverda et al., 1994) have not such a bond, and, in the case of stellacyanin (Strange et al., 1995), the disulfide bridge is in a region of the protein quite different from that of the disulfide bond in azurin. However, simple structural considerations can be misleading in estimating the stability of a protein. The knowledge of the energetics of the protein is also required. The thermal behavior of wt azurin has been previously investigated by some of us (La Rosa et al., 1995; Guzzi et al., 1996, 1998) from both a spectroscopic and a calorimetric point of view to relate the conformational changes occurring in the active site environment with the conformational changes of the whole protein. If the overall results are taking into account, a protein picture emerges that is consistent with a highly cooperative structure and a multistep unfolding pathway.

In this study, the structural and thermodynamic consequences of the removal of the –SS– bond connecting Cys-3 and Cys-26 in azurin are investigated. Site-directed mutagenesis has been used to replace both cysteines with alanine residues. The combined use of different techniques, such as optical absorption, steady-state fluorescence, circular dichroism (CD), and electron paramagnetic resonance (EPR), allowed us to monitor different regions of the protein and to gain more insight on the structural properties of the native state of the Cys-3Ala/Cys-26Ala (C3A/C26A) azurin mutant.

The results show that the spectroscopic properties of the C3A/C26A azurin mutant are very similar to those of wt azurin, indicating that the double mutation prevents neither the correct folding of the protein nor the formation of the metal-binding site.

The thermal unfolding of the C3A/C26A azurin mutant has been followed by differential scanning calorimetry, optical absorption at $\lambda_{max} = 625$ nm, and fluorescence emission using $\lambda = 295$ nm as excitation wavelength. Moreover, the geometry of the copper site in the denaturated state has been resolved by EPR spectroscopy.

The analysis of the overall experimental data shows that the thermal transition from the native to the denaturated state of the modified azurin is irreversible and scan-rate dependent as in the wt azurin (La Rosa et al. 1995). However, the removal of the disulfide bridge results in a dramatic reduction of the protein stability. In fact, the midpoint transition temperatures registered by the different techniques for C3A/C26A azurin mutant are about 20°C lower than those previously obtained for wt azurin. Similarly, the Gibbs free energy calculated for the disulfide bond deficient protein is half that of the wt protein, suggesting that the presence of the disulfide bridge is an important contributor to the high stability of the wt azurin.

EXPERIMENTAL PROCEDURES

Construction, culturing, and isolation of the C3A/C26A azurin mutant

The C3A and C26A azurin mutations were introduced separately in the azurin gene (Canters, 1987) using the oligonucleotide-directed polymerase chain-reaction mutagenesis (Picard et al., 1994). For the single C3A and C26A mutants, the mutagenesis primer, i.e., 5′CTGGCTGCCGAGGCCTCGGTGGACATC-, 5′ATCACCGTCGACAAGAGCGCTAAGCAGTTCACC- (Eurogentec) have been used, respectively. Subsequently, the DNA fragments containing the mutations have been substituted into the wt gene expression vector. Finally, to generate the double mutant, the two DNA fragments containing the single mutations have been ligated, and the intact reading frame encoding the double mutant has been obtained. The plasmid vector pUC 18-derived bearing the C3A/C26A mutant was used for *Escherichia coli* JM101 transformation and expression. Subsequently, the cells were grown in a fermentor containing 30 L Luria-Bertani medium supplemented with 100 μg/mL ampicillin and 100 μM of IPTG for gene induction. The cells were harvested at the end of the exponential

growth phase. In principle, the protocol for C3A/C26A azurin purification could be kept similar to that of the wt azurin (Van der Kamp et al., 1990). The protein was judged pure based on standard I.E.F gel-electrophoresis.

Differential scanning calorimetry and spectroscopic measurements

Differential scanning calorimetry (DSC) scans were carried out with a SETARAM (Lyon, France) microdifferential scanning calorimeter (microDSC) with stainless steel 1-mL sample cells, interfaced with a BULL 200 Micral computer. The sampling rate was 1 point/s in all measuring ranges. The protein (1.25 mg/mL) was dissolved in 10 mM phosphate buffer at pH = 7.03. The ionic strength was adjusted at 0.1 by sodium chloride. Protein solution pH was adjusted by computer-controlled potentiometric titration. Titrations were performed using Metrohm digital pH meter (mod. 654) equipped with Metrohm 109 glass-saturated calomel microelectrode. The titration cell was thermostatted at 25.0 ± 0.2°C, and all solutions were kept under an atmosphere of nitrogen. The same solution without the protein was used in the reference cell. Both the sample and reference were scanned from 30 to 80°C with a precision of ±0.08°C at the scanning rates of 0.3, 0.5, 0.7, and 1°C/min. The calorimetric scans were carried out under an extra nitrogen pressure of 1.5 bar.

The average level of noise was about ±0.4 μW and the reproducibility at refilling was about 0.1 mJ/K/mL. Calibration in energy was obtained by dissipating a defined amount of energy, electrically generated by an EJ2 SETARAM Joule calibrator, within the sample cell.

To obtain the *Cp* curves, buffer–buffer base lines were recorded at the same scanning rate and then subtracted from sample curves (Sturtevant, 1987; Connelly et al., 1991). All the Cp_{exc} curves were obtained using a fourth-order polynomial fit.

Optical Density (OD) measurements were carried out with a JASCO 7850 spectrophotometer equipped with a Peltier-type thermostatted cell holder, model TPU-436 (precision ±0.2°C) and the EHC-441 temperature programmer. Quartz cuvettes with a 1-cm optical path were used throughout. The temperature of the samples was measured directly by a YSI precision thermistor dipped in the cuvette. The experiments were started 3 min after sample positioning in the thermostatted sample holder at the initial temperature of 30°C. The heating rates were 0.3, 0.5, 0.7, and 1°C/min. Protein concentration was 0.4 mg/mL.

Fluorescence emission curves were acquired with a Perkin-Elmer LS 50B spectrofluorimeter equipped with a Peltier Temperature Programmer PTP-1. The excitation wavelength was 295 nm, while the excitation and emission bandpasses were of 6 and 4 nm, respectively. Temperature was scanned from 30 to 82°C at 1°C/min. The temperature of the samples was measured directly by a YSI precision thermistor dipped in the cuvette. The emission spectra were recorded at the scan speed of 400 nm/min. Protein concentration was 0.4 mg/mL.

CD measurements in the far UV region were performed with a JASCO 700 spectropolarimeter using quartz cuvettes of 1-cm optical path. Azurin concentration was 0.3 mg/mL.

The EPR measurements were carried out with a Bruker ER 200D-SRC X band spectrometer equipped with the ESP 1600 Data System. All the EPR spectra were recorded at 77 K by plunging the sample solutions in a finger dewar containing liquid nitrogen positioned into a TE_{102} cavity. Protein concentration was 4 mg/mL.

All data presented in this paper are the average value of three measurements.

RESULTS AND DISCUSSION

Spectroscopic characterization of C3A/C26A azurin mutant

Spectroscopic techniques are essential tools in the investigation of the structure and dynamics of proteins. In Fig. 2 *a* the UV-Vis spectrum of C3A/C26A azurin mutant (*dashed line*) recorded at room temperature is compared to that of wt azurin (*solid line*). As can be seen, the spectral features of the two proteins are rather similar with absorption maxima at 280 and 625 nm. The intense absorption in the Vis region is usually assigned to a ligand-to-metal charge transfer transition between the S(Cys-112)π and the $d_{x^2-y^2}$ orbital of the Cu(II) ion (Solomon et al., 1992). The similarity of the two spectra suggests that the geometry of the copper environment is preserved in the mutated azurin, and the overlap between the two orbitals involved in the transition is maintained.

Figure 2 *b* shows the steady-state fluorescence emission spectra of wt (*solid line*) and C3A/C26A azurin mutant (*dashed line*) collected through excitation at 295 nm at room temperature. At this excitation wavelength the intensity of fluorescence emission is mainly due to the unique Trp residue of the protein. The spectra, perfectly overlapping, have emission maxima at 308 nm, which is consistent with a hydrophobic environment of the chromophore (Guptasarma, 1997). The similarity of the two spectra suggests that the double mutation does not affect the microenvironment where the emitting Trp residue is located. A similar result is obtained when the Tyr and Phe residues are also excited at 280 nm (data not shown).

In Fig. 2 *c*, the far-UV CD spectrum of C3A/C26A azurin mutant recorded at room temperature (*dashed line*) is compared to that of the wt protein (*solid line*). Both spectra show a strong absorption around 220 nm, which is characteristic of β-structure (Mei et al., 1996). No significant deviation from the spectrum of the wt sample is observed in the mutated protein, indicating that both proteins have comparable secondary structure.

Finally, the EPR spectra at 77 K of wt (*solid line*) and C3A/C26A azurin mutant (*dashed line*) are shown in Fig. 2 *d*. The spectral features are typical of a type-1 copper ion

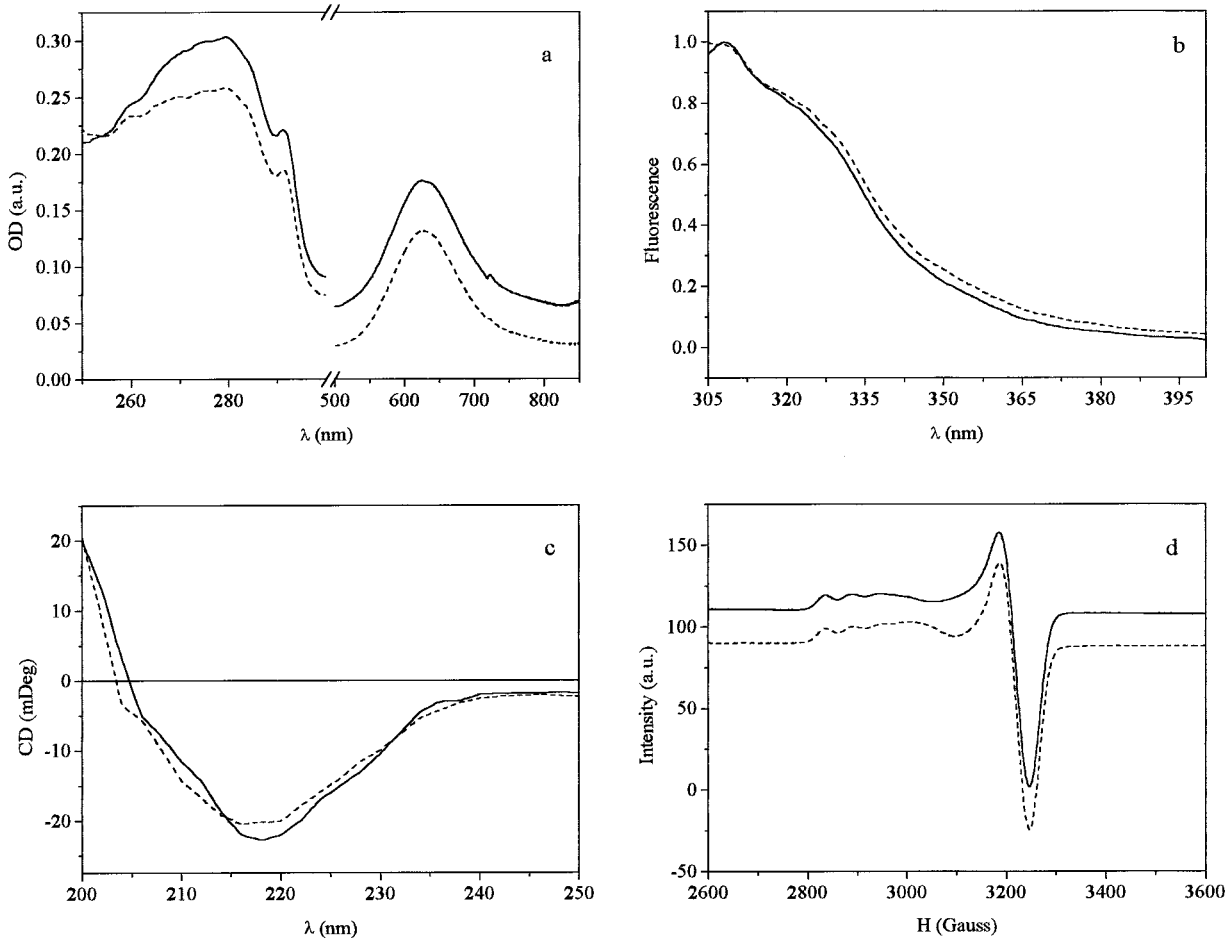

FIGURE 2 (*a*) UV-Vis spectra of wt (*solid line*) and C3A/C26A azurin mutant (*dashed line*) recorded at room temperature. Proteins concentration was 0.4 mg/mL in 10 mM PBS (pH 7.03). (*b*) Normalized fluorescence emission spectra of wt (*solid line*) and C3A/C26A azurin mutant (*dashed line*) in aqueous solution recorded at room temperature through excitation at 295 nm. (*c*) Far-UV CD spectra of wt (*solid line*) and C3A/C26A azurin mutant (*dashed line*) recorded at room temperature. (*d*) Comparison of the EPR spectra of wt (*solid line*) and C3A/C26A azurin mutant (*dashed line*) recorded at 77 K. Proteins concentration was 1 mM in 10 mM PBS (pH 7.03).

with axial symmetry characterized by four hyperfine lines centered at $g_{\|}$ and separated by $A_{\|}$ and by a single, more intense resonance line centered at $g_{\perp}$ at higher fields (Aqualino et al., 1991). The two spectra are very similar, although for the C3A/C26A azurin mutant sample the $m_I = +3/2$ resonance line in the parallel region of the spectrum is centered at a slightly higher magnetic field with respect to the corresponding line in the wt protein.

From the results presented in Fig. 2, it can be concluded that both the copper ion and the Trp environments as well as the secondary and the tertiary structure of the –SS– bond-deficient protein are very similar to those of wt azurin. In other words, the native state of the mutated azurin is not affected in a significant way from the replacement of the two cysteines with alanines. A different result has been previously found on azurin by substituting the two cysteines with serines (Bonander et al., 1995). This mutation gives rise to a significant alteration of the azurin folding and of the metal active site geometry. In fact, the type-1 Cu^{++} is converted into a type-2 copper ion and the fluorescence emission change of the Trp residue shows that it becomes exposed to a polar environment. Moreover, the far-UV CD spectrum of such a mutated azurin indicates a loss of β-structure. This result may be related to the polar character of the serine residues, which can induce a strong pertubation not only on the mutation site but also for the overall protein conformation. Such a perturbation does not occur when the two cysteines are replaced by alanines as in the present study.

Thermal behavior of the C3A/C26A azurin mutant. DSC

In Fig. 3 *a*, the calorimetric profiles of the C3A/C26A azurin mutant and wt azurin recorded in the same experimental conditions are shown. The comparison of the two curves evidences two main differences. The first one is that in the mutated azurin the DSC curve is broad and the temperature of maximum heat absorption, T_{max}, is about

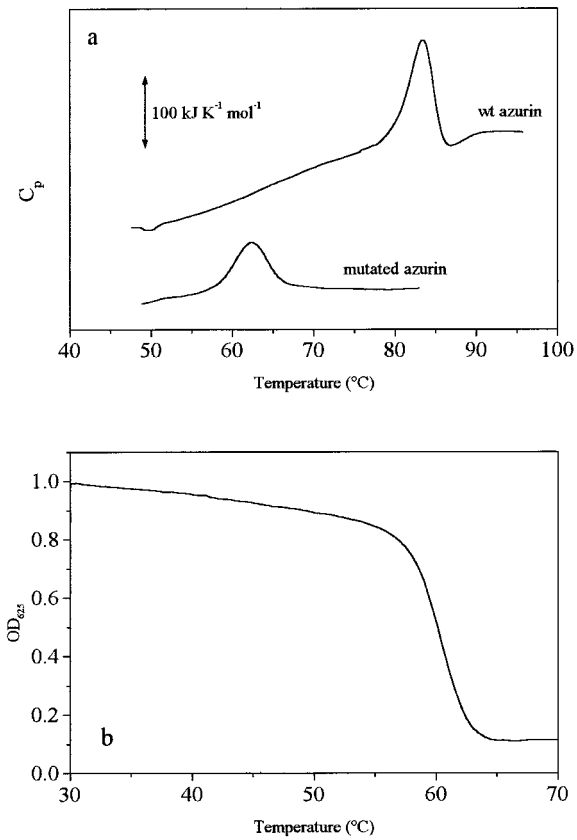

FIGURE 3 (*a*) DSC thermograms of wt and C3A/C26A azurin mutant recorded under the same experimental condition. Protein concentration: 1.25 mg/mL, pH = 7.03, ionic strength 0.1 in NaCl; scan rate 0.5°C/min. (*b*) Normalized OD_{625} versus temperature of C3A/C26A azurin in aqueous solution recorded at a scan rate of 0.5°C/min.

62°C, whereas for the wt protein the same parameter is about 83°C. The broadening of the DSC profile and the reduction of T_{max} suggest a decrease of the cooperativity of the thermal transition and a strong reduction of C3A/C26A azurin mutant stability with respect to the wt protein, respectively. The second difference concerns the intense exothermic peak present at 87°C in the DSC profile of the wt protein, which disappears in the mutated one. This result suggests some differences in the final states reached by the two proteins. Notwithstanding these differences, the thermal unfolding of C3A/C26A azurin mutant is still irreversible like that of the wt protein, i.e., a second scan of a previously scanned sample did not show any endothermic peak. The irreversibility of the thermal transition requires establishment of whether the reaction is under kinetic control, and whether there is a change of molecularity during the heating of the solution (Sanchez-Ruiz, 1992; Galisteo and Sanchez-Ruiz, 1993; Tello-Solis and Hernandez-Harana, 1995). DSC scans at different scan rates allow us to elucidate the first point, whereas a change of molecularity is prevented because azurin is a monomeric protein.

In Table 1 are listed the T_{max} and the experimental ΔH values as a function of the scan rates. As can be seen, T_{max}

TABLE 1 Scanning rate dependence of the optical transition temperature, the maximum heat absorption temperature, and the experimental unfolding enthalpy of C3A/C26A azurin mutant

	Optical Density	Differential Scanning Calorimetry	
Scan/rate (°C/min)	T_t (°C)*	T_{max} (°C)*	ΔH (kJmol^{-1})*
0.3	59.5 ± 0.2	61.22 ± 0.04	344 ± 10
0.5	60.5 ± 0.1	62.15 ± 0.03	405 ± 11
0.7	60.7 ± 0.1	62.95 ± 0.03	385 ± 15
1.0	62.3 ± 0.3	63.81 ± 0.05	335 ± 11
$\infty^{\#}$	—	64.72 ± 0.06	444 ± 18

*Values expressed as mean ± SD.
#Extrapolated values at infinite scan rate.

increases with the scan rate. Such an effect testifies to the irreversible character of the thermal denaturation of the protein. From the scan rate dependence of T_{max}, it is possible to calculate the apparent activation energy, E_{app}, of the denaturation process by using the equation (Sanchez-Ruiz, 1988),

$$\ln\left(\frac{v}{T_{max}^2}\right) = C - \frac{E_{app}}{RT_{max}}, \quad (1)$$

where v is the scan rate (°C/min). From the slope of the linear plot of $\ln(v/T_{max}^2)$ versus $1/T_{max}$, we obtain $E_{app} = 508$ kJ/mol (correlation coefficient is 0.98).

On the other hand, some differences in the values of the denaturation enthalpy measured at varying scan rates are observed (Table 1) in agreement with other works (Sanchez-Ruiz et al., 1988; Grasso et al., 1995; Lyubarev et al. 1998). From a microscopic point of view, the reasons for these differences remain unclear. In principle, the denaturation enthalpy should not depend on the scanning rate, supposing the protein concentration and the initial and final states are identical in all the experiments performed with varying scanning rates. If we assume accurate sample preparation and the similarity of the initial states, it can be hypothesized that the differences registered for ΔH can be attributed to differences in the final states reached by varying the scan rates. Such a situation is realized, for example, when denaturation is accompanied by the formation of aggregates whose characteristics depend on the rate of denaturation, i.e., on the scan rates. The ΔH values obtained for the C3A/C26A azurin mutant (Table 1) are lower than those found for wt protein (La Rosa et al., 1995). This result is in agreement with the idea that the presence of a disulfide bond represents a constraint for the protein structure even in the unfolded state. As a consequence, the hydrogen bonding network in such a system is less favorable than in an unconstrained system. Moreover, the van der Waals' interactions between nonpolar groups, which are highly dependent on the distance, may also be disrupted by the introduction of an –SS– bond (Doig and Williams, 1991). Thus the

ΔH of unfolding is expected to increase in the presence of the disulfide bridge.

In general, the main problem concerning irreversible thermal transitions is that they cannot be analyzed in the light of classical thermodynamics. Then, the knowledge of the energetics of the system requires the use of theoretical models that describe the unfolding pathway. In previous papers authored by some of us (Milardi et al., 1994; La Rosa et al., 1995, 1998; Guzzi et al., 1998), we have developed a model to extract thermodynamic information from irreversible calorimetric data. According to this method, which has been already applied to wt azurin, the whole denaturation process of the C3A/C26A azurin mutant can be described as the sum of two steps: the first (unfolding) is reversible and contains thermodynamic details about the energetics of the protein; the second is irreversible and time dependent. The whole denaturation pathway can be summarized as

$$\mathrm{N} \underset{\Delta H_U,\, T_{1/2}}{\overset{K}{\Leftrightarrow}} \mathrm{U} \underset{\Delta H_F,\, T^*}{\overset{k}{\Rightarrow}} \mathrm{F}$$

where N, U, and F are the native, unfolded, and final states, ΔH_U and ΔH_F are the enthalpy associated with the reversible and the irreversible steps, respectively, $T_{1/2}$ and T^* are the temperatures at which the equilibrium constant, K, and the kinetic constant, k, approach the unity value, respectively. The reversible component can be separated from the irreversible one by using an extrapolation procedure of the Cp_{exc} curve at infinite scanning rate. According to this procedure, we have obtained $\Delta H_U = 444 \pm 18$ kJmol^{-1} and $T_{1/2} = 64.72 \pm 0.06$°C. The details of the extrapolation procedure have been reported elsewhere (La Rosa et al., 1995).

To determine the thermodynamic and the kinetic parameters of the two steps of the denaturation process, the experimental DSC curves of C3A/C26A azurin, obtained at different scan rates, were simulated with the equation,

$$Cp_{exc} = \left[\frac{K\Delta H_U}{(K+1)^2} \left\{ \frac{k}{v} + \frac{\Delta H_U}{RT^2} \right\} + \Delta H_F \frac{1}{v} \frac{kK}{K+1} \right] \exp\left\{ -\frac{1}{v} \int_{T_0}^{T} \frac{kK}{K+1}\, dT \right\}, \quad (2)$$

where the previously determined quantities ΔH_U and $T_{1/2}$ have been used as starting values, R being the gas constant, T_0 is the onset temperature of denaturation, and

$$K = \exp\left\{ -\frac{\Delta H_U}{R} \times \left(\frac{1}{T} - \frac{1}{T_{1/2}} \right) \right\}, \quad (3)$$

$$k = \exp\left\{ -\frac{E}{R} \times \left(\frac{1}{T} - \frac{1}{T^*} \right) \right\}, \quad (4)$$

where E is the activation energy of the irreversible step.

This equation, which originates from the classical Lumry–Eyring model, has been previously improved (Milardi et al., 1994) by considering the enthalpy, ΔH_F, of the U $\Rightarrow$ F process not negligible. The unknown parameters ΔH_F, T^* and E have been obtained from the fitting procedure. In Fig. 4 the experimental heat capacity curve of C3A/C26A azurin mutant recorded at 0.5°C/min (*solid line*) is compared with the corresponding curve obtained by using Eq. 2 (*dashed line*). The two curves are in good agreement. This suggests that the proposed model provides a reliable description of the thermal denaturation of C3A/C26A azurin mutant.

Optical density

The variation of the intense optical absorption at 625 nm as a function of temperature can be used to directly monitor the local conformational changes occurring in the copper environment when the temperature increases. Because the copper ion is located in a hydrophobic region of the protein, these changes reflect those occurring in the tertiary or secondary structure of the protein. Figure 3 *b* shows the normalized optical density at 625 nm, OD_{625}, in the temperature range 30–70°C of C3A/C26A azurin mutant in aqueous solution recorded at the scan rate of 0.5°C/min. The thermal profile shows a transition temperature, T_t, defined as the midpoint of the OD transition, of 59.5°C. This T_t value is remarkably lower than the corresponding one shown from the wt protein (T_t = 79.3°C) and reflects the strong decrease in stability of the mutated azurin. After the thermal denaturation, the characteristic blue color of the protein is not recovered by cooling back the solution to room temperature. Such an effect can be ascribed to conformational changes of the tertiary structure of the protein, which permanently alter the copper coordination environment (see also the section Electron Paramagnetic Resonance).

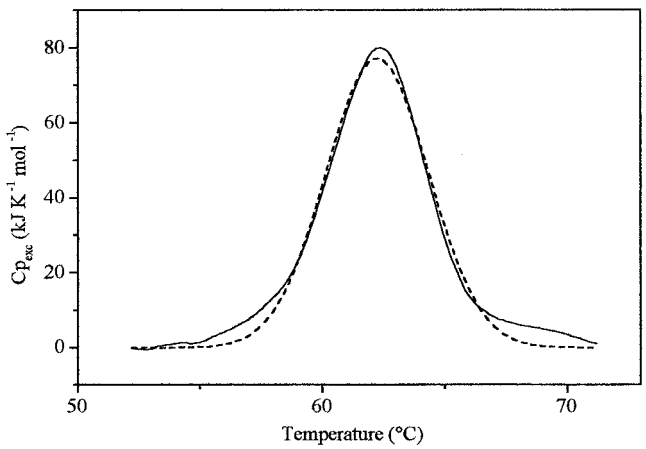

FIGURE 4 Curve fitting with Eq. 2 of the experimental Cp_{exc} profile recorded at 0.5°C/min. The starting values were ΔH_U = 444 kJ/mol and $T_{1/2}$ = 64.7°C.

The occurrence of kinetic factors in the thermal disruption of the active site of C3A/C26A azurin mutant has been verified by performing OD_{625}/T measurements at different scan rates. The T_t values obtained at 0.3, 0.5, 0.7, and 1.0°C/min are listed in Table 1. As can be inferred from the data, T_t increases with the scan rate according to the trend observed in the DSC scans. The comparison of T_t and T_{max} shows that T_t has always a slight lower value with respect to T_{max}. The difference, $\Delta T = T_{max} - T_t > 0$ for each scan rate, suggests that the disruption of the active site precedes the whole protein denaturation.

The scan rate dependence of T_t can be used to calculate the activation energy, E_a, of the denaturation process using Eq. 1, where E_{app} and T_{max} are now substituted by E_a and T_t, respectively. The result of the fit of the experimental points with Eq. 1 gives an E_a value of 460 ± 8 kJmol^{-1}, which is comparable, within the experimental error, with the value registered for the wt protein (La Rosa et al., 1995).

Electron paramagnetic resonance

Figure 5 shows the EPR spectra of C3A/C26A azurin mutant in aqueous solution recorded at 77 K after the protein solution has been heated at 75 (*curve a*) and 90°C (*curve b*) for 10 min. The first temperature has been chosen above the end of the DSC thermal transition. The EPR spectrum, when compared to the magnetic signal recorded on the native state of C3A/C26A azurin mutant (Fig. 2 *d*, *dashed line*), shows a strong temperature-induced effect both on the copper-ligands geometry and coordination atoms. In fact, the copper-ligand geometry undergoes a transition from trigonal bipyramidal in the native state to square planar in the final state as testified from the change of the $A_{//}$ value from 55 to 175 Gauss. Moreover, in the high magnetic field region of the spectrum, traces of a superhyperfine structure are evident (Fig. 5, *curve a*). A better resolution of this superhyperfine structure can be observed in the spectrum recorded after heating the C3A/C26A azurin mutant solution at 90°C (Fig. 5, *curve b*). The superhyperfine structure arises from the interaction of the unpaired electron spin of the Cu^{++} ion with the nuclear spin of the ligand atoms (McGarvey, 1967). This result is quite different from that previously obtained for wt protein (see Fig. 8 in La Rosa et al., 1995). In fact, although in both cases the final geometry can be assimilated to square planar, an increase in the hyperfine splitting from 160 Gauss in the denaturated wt azurin to 175 Gauss in denaturated C3A/C26A azurin mutant is registered. The differences observed in the EPR spectra of the denaturated state of wt and C3A/C26A azurin mutant suggest that the mutation affects the final conformational state reached by the protein in absence of the disulfide bridge. In particular, the presence of at least nine superhyperfine resonance lines suggests that there are four nitrogen atoms in the copper coordination sphere of the denaturated C3A/C26A azurin mutant. In contrast to this, two N and two O ligands had been proposed for the copper coordination of the denaturated state of wt protein (La Rosa et al., 1995).

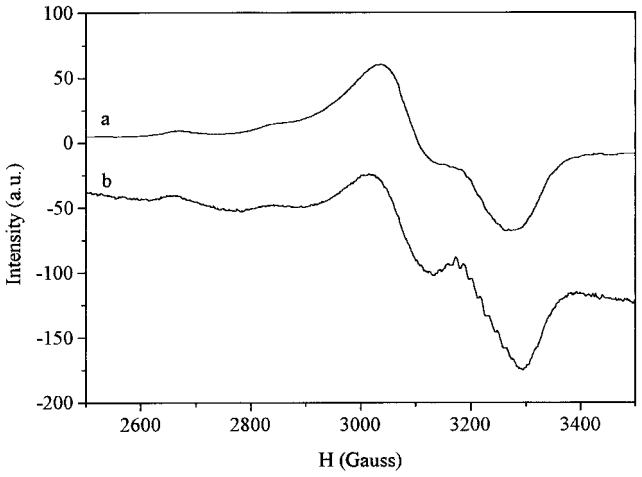

FIGURE 5 EPR spectra of C3A/C26A azurin mutant recorded at 77 K after heating of the sample solution for 10 min at 75°C (*curve a*) and 90°C (*curve b*).

Fluorescence emission

The fluorescence emission signal of the Trp residue in a protein is closely related to its solvent exposure (Lakowicz, 1986), so that the Trp emission spectra can provide useful information about the changes of the protein conformational states. The fluorescence spectra of the wt and C3A/C26A azurin mutant collected through excitation at 295 nm have been recorded in steps of 1°C in the temperature range 30–82°C. The inset of Fig. 6 shows, as an example, the fluorescence spectra of C3A/C26A azurin mutant recorded at 30 and 62°C. At low temperature, the maximum emission is at 308 nm, whereas at high temperature it occurs at 357 nm. The same results are also observed for wt azurin at 30 and 80°C, respectively. The first wavelength is compatible with a Trp residue completely buried in the interior of the protein and surrounded by nonpolar amino acid residues (Lakowicz, 1986). The second one being compatible with the fluorescence emission of a Trp residue exposed to the aqueous solvent (Guptasarma, 1997).

In Fig. 6 the variations of the fluorescence emission intensity at 308 and 357 nm as a function of temperature for wt and C3A/C26A azurin mutant are reported. As can be seen, the effect of the temperature on the fluorescence intensity is similar in both proteins. In fact, with temperature increase, a reduction of the fluorescence intensity at 308 nm is observed, then the maximum emission wavelength shifts at 357 nm, and an increase in the fluorescence intensity occurs, too. However, the transition temperature, defined as the midpoint of the fluorescence variation at 308 nm, is 78°C for wt protein and 58°C for the mutated azurin. These findings further support the results obtained using the other experimental techniques and confirm the strong reduction of stability of azurin upon removal of the –SS– bond.

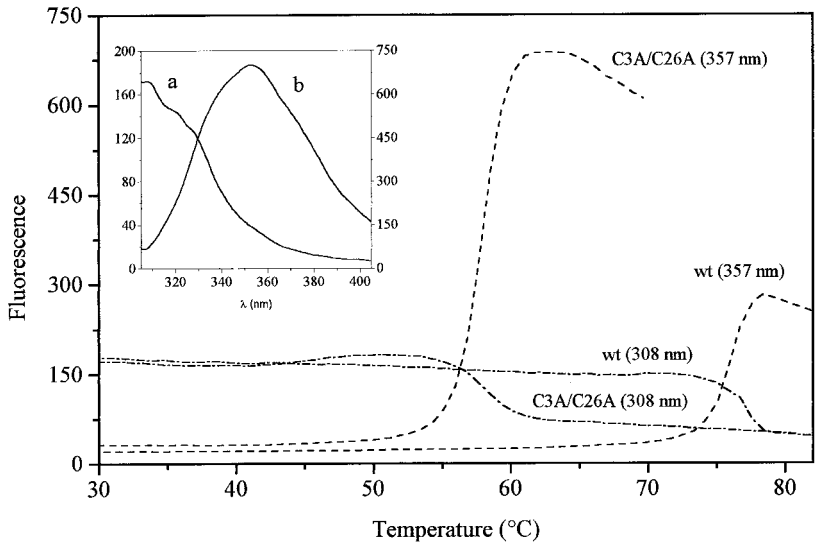

FIGURE 6 Temperature-dependent fluorescence emission of wt and C3A/C26A azurin mutant at λ_{308} and λ_{357}. λ_{exc} = 295 nm. Protein concentration was 0.4 mg/mL in 10 mM PBS (pH 7.03). *Inset:* Fluorescence emission spectra of C3A/C26A azurin mutant recorded at 30 (*curve a*) and 62°C (*curve b*). The vertical axis of the fluorescence intensity on the left refers to sample (*a*) and that on the right to sample (*b*).

Because the solvent accessibility is the major factor determining the fluorescence of the Trp residue, the data in Fig. 6 suggest that the fluorescence change may reach its limiting value before both proteins fully unfold. In fact, the temperatures of 78 and 58°C, determined by means of fluorescence emission for wt and C3A/C26A azurin mutant, respectively, are lower than those extracted from the DSC profiles (Fig. 3 *a*). In addition, the comparison between the fluorescence emission and optical absorption data reveals that the solvent exposure of the Trp residue occurs before the disruption of the copper site.

It is noteworthy that the Trp fluorescence intensity at 357 nm increases upon unfolding. Moreover, the fluorescence intensity of C3A/C26A azurin in the denaturated state is much higher than the corresponding one of the wt protein. This result supports the hypothesis that the conformational states of the two proteins after the thermal denaturation are quite different. In fact, because the Trp fluorescence in holo-azurin is extensively quenched compared to that of copper-depleted azurin (Petrich et al., 1987; Hansen et al., 1990; Sweeney et al., 1991), it turns out that the fluorescence emission intensity gain of the C3A/C26A azurin mutant may be related to a marked increase in the Cu–Trp-48 distance. On the other hand, this finding is consistent with EPR data that show a tight binding of the copper ion with ligand atoms in the denaturated-mutated azurin, which are different with respect to the wt protein.

Thermodynamic analysis of the unfolding process

The calculation of the Gibbs free energy relative to the unfolding process in all the temperature range considered requires the knowledge of three parameters: ΔH_U, $T_{1/2}$, and ΔCp. Unfortunately, the irreversibility of the thermal transition of the C3A/C26A azurin mutant prevents the experimental determination of $\Delta Cp = Cp_U - Cp_N$, because the value of Cp at the offset temperature is ascribable to the final (F) state and not to the unfolded (U) one. To solve this problem, both alternative experimental methods and theoretical models can be used. In this paper, the calculation of ΔCp has been obtained by three different approaches. In the first one, the denaturational ΔCp is obtained from the temperature dependence of the unfolding enthalpy ΔH_U using the Kirchhoff equation. Several sets of calorimetric experiments have been carried out at different pH values from 4.8 to 7.0. Then the ΔH_U and the $T_{1/2}$ values, related to the thermally induced unfolding of C3A/C26A azurin mutant, have been calculated following the extrapolation procedure at infinite scanning rate (La Rosa et al., 1995). The temperature dependence of the extrapolated unfolding enthalpies ΔH_U obtained at different pH values is linear with $T_{1/2}$. The slope of the linear fit gives 8.9 ± 0.9 $kJK^{-1}mol^{-1}$ for the heat capacity changes upon unfolding of C3A/C26A azurin mutant in H_2O.

The second approach consists in the use of the Murphy and Gill (1991) model. According to this model, the ΔCp value can be evaluated on the basis of the set of equations,

$$\Delta Cp = \Delta Cp_{ap} + \Delta Cp_{pol}, \quad (5)$$

$$\Delta Cp_{ap} = f_{ap} \times N_{CH} \times (\Delta C^0)p_{\text{-CH-}}, \quad (6)$$

$$f_{ap} = 0.574 + 0.000702 \times N_{res}, \quad (7)$$

$$\Delta Cp_{pol} = 0.73 \times N_{res} \times (\Delta C^0)p_{\text{-CONH-}}, \quad (8)$$

$$(\Delta C^0)p_{\text{-CONH-}} = -60 \pm 6\ JK^{-1}mol^{-1}, \quad (9)$$

$$(\Delta C^0)p_{\text{-CH-}} = 28 \pm 1\ JK^{-1}mol^{-1}, \quad (10)$$

where ΔCp_{ap} is the denaturational heat capacity change ascribable to apolar groups, ΔCp_{pol} is the heat capacity change ascribable to polar groups, f_{ap} is the fraction of apolar buried surface area, N_{res} is the number of the residues in the protein, N_{CH} is the number of apolar hydrogen atoms (i.e., the hydrogen atoms directly bound to a carbon atom),

$(\Delta C^0)p_{\text{-CH-}}$ is the specific contribution of one mole of apolar hydrogens to the overall denaturational heat capacity change and $(\Delta C^0)p_{\text{-CONH-}}$ is the specific contribution ascribable to one mole of polar residues (Murphy and Gill, 1991). Because there are 759 apolar hydrogen atoms and 128 aminoacid residues in C3A/C26A azurin mutant, ΔCp is 8.5 ± 1.0 kJK^{-1}mol^{-1}.

The third method is based on the average properties of globular proteins (Milardi et al., 1997). This method starts from the correlation of ΔCp with N_{res} and N_{CH} of well-known globular proteins at various temperatures. According to this method, we obtain a ΔCp value of 7.9 kJK^{-1}mol^{-1} and in the temperature range 20–100°C the ΔCp variation is ± 1.0 kJK^{-1}mol^{-1}.

To minimize the errors, ascribable either to experimental uncertainties or to the nonperfect efficiency of the models, the ΔCp used to calculate the thermodynamic functions has been taken as the average of the three values, which corresponds to 8.4 ± 1.0 kJK^{-1}mol^{-1}. This value is also in good agreement with the ΔCp value calculated according to the equation (Doig and Williams, 1991),

$$\Delta Cp = 77N_{\text{res}} - 940N_{\text{ss}} \text{ JK}^{-1}\text{mol}^{-1}, \tag{11}$$

where N_{ss} is the number of disulfide bridges. The ΔCp obtained is 8.9 kJK^{-1}mol^{-1}. The denaturational heat capacity change, together with $T_{1/2} = 64.72$°C and $\Delta H_{\text{U}} = 444$ kJmol^{-1} values, allow us to calculate $\Delta H(T)$, $\Delta S(T)$, and $\Delta G(T)$, characterizing the thermal behavior of C3A/C26A azurin mutant by using the equations

$$\Delta H(T) = \Delta H_{\text{U}} - \Delta Cp(T_{1/2} - T), \tag{12}$$

$$\Delta S(T) = \frac{\Delta H_{\text{U}}}{T_{1/2}} - \Delta Cp \ln \frac{T_{1/2}}{T}, \tag{13}$$

$$\Delta G(T) = \Delta H_{\text{U}} \frac{T_{1/2} - T}{T} - \Delta Cp(T_{1/2} - T) + T\Delta Cp \ln \frac{T_{1/2}}{T}. \tag{14}$$

The three functions are drawn in Fig. 7. In the same figure, the previously thermodynamic functions related to the thermal denaturation of wt azurin in H_2O (La Rosa et al., 1995) are also shown.

By comparing the two ΔG functions (Fig. 7 *c*), it can be seen that the temperature of maximum stability is about 20°C in both cases. Moreover, $\Delta\Delta G = \Delta G_{\text{wt}} - \Delta G_{\text{-SS-}} \cong 27$ kJmol^{-1} is constant over the whole temperature range (the subscript indexes wt and –SS– refer to wt and disulfide-deficient azurin). This result suggests that the presence of the disulfide bridge in the wt azurin contributes significantly to the stability of the protein and is not temperature dependent. If we consider the enthalpic contribution (Fig. 7 *a*) to ΔG, it can be seen that ΔH_{wt} and $\Delta H_{\text{-SS-}}$ coincide in all the temperature range. The close similarity of the unfolding enthalpy value of the two proteins suggests that the reduced stability of C3A/C26A azurin mutant arises mainly from entropic effects. This result is in agreement with a DSC study of wt and three-disulfide lysozyme derivative (Cooper et al., 1992). An opposite conclusion has been proposed by Doig and Williams (1991) based on the correlations between the thermodynamic properties and the number of the disulfide bridges present in six proteins.

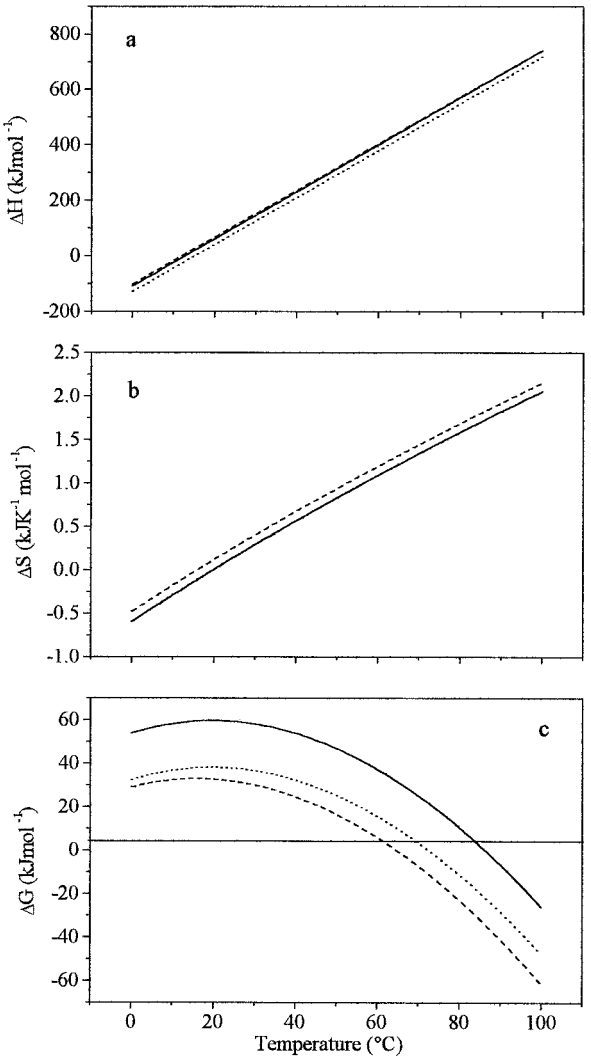

FIGURE 7 Temperature dependence of the unfolding (*a*) enthalpy, (*b*) entropy, and (*c*) Gibbs free energy for wt (*solid line*), C3A/C26A azurin mutant (*dashed line*). The thermodynamic functions expected using the Murphy and Gill model (see the text for details) are also shown (*dotted line*).

A different behavior is observed in the entropic component. ΔS_{wt} is less than $\Delta S_{\text{-SS-}}$ over the whole temperature range (Fig. 7 *b*). In particular, at 20°C, the entropy of unfolding of C3A/C26A azurin mutant is about 115 JK^{-1}mol^{-1} higher than that of the wt protein (Table 2). This is consistent with the increase in the conformational entropy in the unfolded polypeptide chain resulting from removal of the –SS– cross-link (Vogl et al., 1995). Based on a series of studies on a large variety of proteins, it has been shown that this entropic contribution depends on the size of the loop connecting the –SS– bond according to the equation (Pace

TABLE 2 Thermodynamic parameter values of wt (Milardi et al., 1996), C3A/C26A azurin mutant and calculated (Model) by using Murphy and Gill method at the temperature of maximum stability (20°C)

	ΔH ($kJmol^{-1}$)	ΔS ($kJK^{-1}mol^{-1}$)	$T\Delta S$ ($kJmol^{-1}$)	ΔG ($kJmol^{-1}$)
Azurin wt	61.0 ± 6.7	0.0045 ± 0.0005	1.3 ± 0.1	59.7 ± 6.5
C3A/C26A	67.1 ± 5.4	0.12 ± 0.01	35.2 ± 2.8	32.6 ± 2.6
Model	40.5 ± 3.2	0.008 ± 0.006	2.3 ± 0.2	38.1 ± 3.0

et al., 1988; Vogl et al., 1995),

$$\Delta S_{conf} = 8.8 + 1.5R \ln(n) JK^{-1}mol^{-1}, \quad (15)$$

where R is the gas constant and n is the number of residues in the loop. In azurin, the removal of the disulfide bridge should provide an increase in conformational entropy of 47.9 $JK^{-1}mol^{-1}$. Experimental data reported in Table 2 show that the removal of the disulfide bridge in azurin implies an entropy gain of 115 $JK^{-1}mol^{-1}$ on unfolding. By subtracting from this value the conformational entropy, we obtain the residual entropy, ΔS_{res}, which is 67.1 $JK^{-1}mol^{-1}$. This residual entropy can be ascribed both to solvent-related effects that operate via a decrease in the water-exposed nonpolar surface area of the unfolded protein and to changes in the Cu coordination sphere in the unfolded mutant and wt protein (see Fig. 5). For some proteins, it has been shown that ΔS_{res} can be calculated by means of the equation (Doig and Williams, 1991),

$$\Delta S_{res} = 2N_{res} + 290N_{ss} JK^{-1}mol^{-1}. \quad (16)$$

According to this point of view, the ΔS_{res} for azurin should be 34 $JK^{-1}mol^{-1}$, which is lower than the expected value (67.1 $JK^{-1}mol^{-1}$). Hence, we believe that, in the case of azurin, other factors contribute positively to the entropic increase after removal of the disulfide bridge. We suggest that additional entropic factors can arise from a decrease of the entropy of the native state of the mutated azurin as a consequence of a modified hydrogen bonds network and nonpolar intramolecular interactions due to the removal of the disulfide bridge.

At a first approximation, the effect of the metal ion on unfolding can also be considered by comparing the ΔG values calculated for the C3A/C26A azurin mutant and the one expected from applying the Murphy and Gill (1991) model, where the average thermodynamic features of proteins are considered only in terms of polar and apolar groups, i.e., neither the metal ion nor the –SS– bridge are considered. From the curves shown in Fig. 7 *c* it seems that the simultaneous absence of both the disulfide bridge and the Cu^{++} ion makes the protein more stable by about 6 $kJmol^{-1}$ with respect to the absence of the only –SS– cross-link. Structural details can be invoked to explain the different behavior of the thermodynamic functions, in particular of the entropic destabilization, in the mutated azurin with respect to the wt protein. The native structure of azurin is very compact, and as a consequence, the introduction of a disulfide bond in such a structure may induce only negligible effect on the entropy of the native state of the protein. In contrast, the number of the possible conformations that the protein can assume in the final state may be significantly lower if an –SS– bond is present as in the wt azurin. As a consequence, $\Delta S_{wt} < \Delta S_{\text{-SS-}}$. This hypothesis is also supported by the EPR and fluorescence emission measurements where differences in the final state of wt and C3A/C26A azurin mutant have been evidenced.

CONCLUSIONS

The results presented in this study show that the double substitution of Cys-3 and Cys-26 with alanine residues does not affect the spectral properties and the most structural features of C3A/C26A azurin mutant with respect to the wt protein, whereas the thermodynamic consequences of the removal of the disulfide bond are considerable. The reduced stability of the C3A/C26A azurin mutant is evident from both the downward shift of the transition temperature from the native to the denaturated state of the protein as well as from the decrease of the ΔG value. This reduction has mainly an entropic character. The presence of the disulfide bridge stabilizes the protein in two ways: 1) it decreases the conformational entropy of the unfolded state, and 2) it increases the surface area exposed to the solvent on unfolding of the nonpolar residues of the protein. In the case of azurin, these two entropic effects have almost the same weight, whereas the removal of the disulfide cross-link has little effect on the enthalpy of denaturation of the protein.

The different techniques used in this paper also allow us to hypothesize a sequence of events in the thermal denaturation process of azurin, which starts with the destabilization of the Trp environment, proceeds through the disruption of the copper site, and then the whole protein molecule collapses in the denaturated state.

One of us (R.G.) thanks the University of Calabria for a post-doctoral fellowship. This work has been supported by the Ministero dell' Università e della Ricerca Scientifica e Tecnologica, Consiglio Nazionale delle Ricerche, Istituto Nazionale di Fisica della Materia, and Consorzio Interuniversitario Biotecnologie.

REFERENCES

Aqualino, A., A. S. Brill, G. F. Bryce, and B. S. Gerstman. 1991. Correlated distribution in g and A tensors at a biologically active low-symmetry cupric site. *Phys. Rev. A*. 44:5257–5271.

Bonander, N., B. G. Karlsson, and T. Vänngård. 1995. Disruption of the disulfide bridge in azurin from *Pseudomonas aeruginosa*. *Biochim. Biophys. Acta*. 1251:48–54.

Canters, G. W. 1987. The azurin gene from *Pseudomonas aeruginosa* codes for a pre-protein with a signal peptide. *FEBS Lett.* 212:168–172.

Clarke, J., and A. R. Fersht. 1993. Engineering disulfide bonds as probes of the folding pathway of barnase: increasing the stability of proteins against the rate of denaturation. *Biochemistry*. 32:4322–4329.

Connelly, P., L. Ghosaini, C. Q. Hu, S. Kitamura, A. Tanaka, and J. M. Sturtevant. 1991. A differential scanning calorimetric study of the thermal unfolding of seven mutant forms of Phage T4 lysozyme. *Biochemistry.* 30:1887–1895.

Cooper, A., S. J. Eyles, S. E. Radford, and C. M. Dobson. 1992. Thermodynamic consequences of the removal of a disulfide bridge from hen lysozyme. *J. Mol. Biol.* 225:939–943.

Creighton, T. E. 1974. Intermediates in the refolding of reduced bovine pancreatic trypsin inhibitor. *J. Mol. Biol.* 87:579–602.

Creighton, T. E. 1992. Folding pathways determined using disulfide bonds. *In* Protein Folding. T. E. Creighton, editor. W. H. Freeman and Co., New York. 301–351.

Doig, A. J., and D. H. Williams. 1991. Is the hydrophobic effect stabilizing or destabilizing in proteins? The contribution of disulphide bonds to protein stability. *J. Mol. Biol.* 217:389–398.

Galisteo, M. L., and J. M. Sanchez-Ruiz. 1993. Kinetic study into the irreversible thermal denaturation of bacteriorhodopsin. *Eur. Biophys. J.* 22:25–30.

Gokhale, R. S., S. Agarwalla, V. S. Francis, D. V. Santi, and P. Balaram. 1994. Thermal stabilization of thymidylate synthase by engineering two disulfide bridges across the dimer interface. *J. Mol. Biol.* 235:89–94.

Grasso, D., C. La Rosa, D. Milardi, and S. Fasone. 1995. Effect of scan rate and protein concentration on DSC thermograms of bovine superoxide dismutase. *Thermochim. Acta*. 265:163–175.

Guptasarma, P. 1997. Resolving multiple protein conformers in equilibrium unfolding reactions: a time-resolved emission spectroscopic (TRES) study of Azurin. *Biophys. Chem.* 65:221–228.

Guss, J. M., H. D. Bartunik, and H. C. Freeman. 1992. Accuracy and precision in protein structure analysis: restrained least-squares refinement of the structure of poplar plastocyanin at 1.33 Å resolution. *Acta Cryst.* B48:790–811.

Guzzi, R., C. La Rosa, D. Grasso, D. Milardi, and L. Sportelli. 1996. Experimental model for the thermal denaturation of azurin: a kinetic study. *Biophys. Chem.* 60:29–38.

Guzzi, R., L. Sportelli, C. La Rosa, D. Grasso, and D. Milardi. 1998. Solvent isotope effects on azurin thermal unfolding. *J. Phys. Chem. B* 102:1021–1028.

Hansen, J. E., J. W. Longworth, and G. R. Fleming. 1990. Photophysics of metalloazurin. *Biochemistry.* 29:7329–7338.

Inaka, K., Y. Taniyama, M. Kikuchi, K. Morikawa, and M. Matsushima. 1991. The crystal structure of a mutant human lysozyme C77/95A with increased secretion efficiency in yeast. *J. Biol. Chem.* 266: 12599–12603.

Kalverda, A. P., S. S. Wymenga, A. Lommen, F. J. M. van de Ven, C. W. Hilbers, and G. W. Canters. 1994. Solution structure of the type 1 blue copper protein Amicyanin from *Thiobacillus versutus*. *J. Mol. Biol.* 240:358–371.

Kraulis, P. J. 1991. MOLSCRIPT: a program to produce both detailed and schematic plots of protein structures. *J. Appl. Cryst.* 24:946–950

Lakowicz, J. R. 1986. Principles of Fluorescence Spectroscopy. Plenum Press, New York and London.

La Rosa, C., D. Grasso, D. Milardi, R. Guzzi, and L. Sportelli. 1995. Thermodynamics of the thermal unfolding of azurin. *J. Phys. Chem.* 99:14864–14870.

La Rosa, C., D. Milardi, and D. Grasso. 1998. Thermodynamics and kinetics of globular protein thermal unfolding. *Recent Res. Devel. Phys. Chem.* 2:175–202.

Lyubarev, A. E., B. I. Kurganov, A. A. Burlakova, and V. N. Orlov. 1998. Irreversible thermal denaturation of uridine phosphorylase from *Escherichia coli* K-12. *Biophys. Chem.* 70:247–257.

McGarvey, B. R. 1967. Electron spin resonance of transition metal complexes.*In* Transition Metal Chemistry. Vol. 3. R. Carlin, editor. M. Dekker, New York. 90–201.

Matsumura, M., W. Becktel, M. Levitt, and B. W. Matthews. 1989. Stabilization of phage T4 lysozyme by engineered disulfide bonds. *Proc. Natl. Acad. Sci. USA.* 86:6562–6566.

Mei, G., G. Gilardi, M. Venanzi, N. Rosato, G. W. Canters, and A. Finazzi Agrò. 1996. Probing the structure and mobility of *Pseudomonas aeruginosa* azurin by circular dichroism and dynamic fluorescence anisotropy. *Protein Sci*. 5:2248–2254.

Milardi, D., C. La Rosa, and D. Grasso. 1994. Extented theoretical analysis of irreversible protein thermal unfolding. *Biophys. Chem.* 52:183–189.

Milardi, D., S. Fasone, C. La Rosa, and D. Grasso. 1996. Contribution of polar and apolar groups to the thermodynamic stability of azurin. *Il Nuovo Cimento*. 18:1347–1353

Milardi, D., C. La Rosa, S. Fasone, and D. Grasso. 1997. An alternative approach in the structure-based prediction of the thermodynamics of protein unfolding. *Biophys. Chem.* 69:43–51.

Murphy, P. K, and S. J. Gill. 1991. Solid model compounds and the thermodynamics of protein unfolding. *J. Mol. Biol.* 222:699–709.

Nar, H., A. Messerschmidt, and R. Huber. 1991. X-ray crystal structure of the two site-specific mutants His35Gln and His35Leu of azurin from *Pseudomonas aeruginosa. J. Mol. Biol.* 218:427–447.

Pace, C. N., G. R. Grimsley, J. A. Thomson, and B. J. Barnett. 1988. Conformation stability and activity of ribonuclease T1 with zero, one and two intact disulfide bonds. *J. Biol. Chem.* 263:11820–11825.

Petrich, J. W., J. W. Longworth, and G. R. Fleming. 1987. Internal motion and electron transfer in proteins: a picosecond fluorescence study of three homologous azurin. *Biochemistry.* 26:2711–2722.

Picard, P., E. Ersdal-Badju, A. Lu, and S. C. Clark. 1994. A rapid and efficient one tube PCR-based mutagenesis technique using *Pfu* DNA polymerase. *Nucl. Acids Res.* 22:2587–2591.

Privalov, P. L. 1992. Physical basis of the stability of the folded conformations of proteins. *In* Protein Folding. T. E. Creighton, editor. W. H. Freeman and Co., New York. 83–126.

Sanchez-Ruiz J. M. 1992. Theoretical analysis of Lumry–Eyring models in differential scanning calorimetry. *Biophys. J.* 61:921–935.

Sanchez-Ruiz, J. M., J. L. Lopez-Lacomba, M. Cortijo, and P. L. Mateo. 1988. Differential scanning calorimetry of the thermal denaturation of Thermolysin. *Biochemistry*. 27:1648–1652.

Schwarz, H., H.-J. Hinz, A. Mehlich, H. Tschesche, and H. R. Wenzel. 1987. Stability studies on derivatives of the bovine pancreatic trypsin inhibitor. *Biochemistry*. 26:3544–3551.

Solomon, E. I., M. J. Baldwin, and M. D. Lowery. 1992. Electronic structures of active site in copper proteins: contributions to reactivity. *Chem. Rev.* 92:521–542.

Strange, R. W., B. Reinhammar, L. M. Murphy, and S. S. Hasnain. 1995. Structural and spectroscopic studies of the copper site of stellacyanin. *Biochemistry*. 34:220–231.

Sturtevant, J. M. 1987. Biochemical applications of differential scanning calorimetry. *Annu. Rev. Phys. Chem.* 38:463–512.

Sweeney, J. A., P. A. Harmon, S. A. Asher, C. M. Hutnik, and A. G. Szabo. 1991. UV Resonance Raman examination of the azurin tryptophan environment and energy relaxation patways. *J. Am. Chem. Soc.* 113: 7531–7537.

Tamura, A., S. Kojima, K. Miura, and J. M. Sturtevant. 1994. Effect of an intersubunit disulfide bond on the stability of streptomyces subtilisin inhibitor. *Biochemistry*. 33:4512–4520.

Taniyama, Y., Y. Yamamoto, M. Kikuchi, and M. Ikehara. 1988. Role of disulfide bonds in folding and secretion of human lysozyme in *Saccharomyces cerevisiae*. *Biochem. Biophys. Res. Commun.* 152:962–967.

Tello-Solis, S. R., and A. Hernandez-Arana. 1995. Effect of irreversibility on the thermal denaturation of *Aspergillus satoi* acid proteinase. *Biochem. J.* 311:969–974.

Van de Kamp, M., F. C. Hali, N. Rosato, A. Finazzi-Agro, and G. W. Canters. 1990. Purification and characterization of a non-reconstitutable azurin. *Biochem. Biophys. Acta.* 1019:283–292.

Vogl, T., R. Brengelmann, H.-J. Hinz, M. Scharf, M. Lotzbeyer, and J. W. Engels. 1995. Mechanism of protein stabilization by disulfide bridges:

calorimetric unfolding studies on disulfide-deficient mutants of the α-amylase inhibitor Tendamistat. *J. Mol. Biol.* 254:481–496.

Wetzel, R., L. J. Perry, W. A. Baase, and W. J. Becktel, 1988. Disulfide bonds and thermal stability in T4 lysozyme. *Proc. Natl. Acad. Sci. USA.* 85:401–405.

Wetzel, R. 1987. Harnessing disulfide bonds using protein engineering. *Trends Biochem. Sci.* 12:478–482.

White, F. H., Jr. 1982. Studies on the relationship of disulfide bonds to the formation of the secondary structure in chicken egg white lysozyme. *Biochemistry*. 21:967–977.